Hypertension Research (2021) 44:1261–1273
https://doi.org/10.1038/s41440-021-00700-7

ARTICLE

Rivaroxaban attenuates cardiac hypertrophy by inhibiting protease-activated receptor-2 signaling in renin-overexpressing hypertensive mice

Masato Narita[1] · Kenji Hanada[1] · Yosuke Kawamura[1] · Hiroaki Ichikawa[1] · Shuntaro Sakai[1] · Yoshikazu Yokono[1] · Maiko Senoo[1] · Noritomo Narita[1] · Michiko Shimada[1] · Tomohiro Osanai[2] · Ken Okumura[3] · Hirofumi Tomita[1]

Received: 3 August 2020 / Revised: 7 March 2021 / Accepted: 28 March 2021 / Published online: 20 July 2021

Abstract

Rivaroxaban (Riv), a direct factor Xa (FXa) inhibitor, exerts anti-inflammatory effects in addition to anticoagulation. However, its role in cardiovascular remodeling is largely unknown. We tested the hypothesis that Riv attenuates the progression of cardiac hypertrophy and fibrosis induced by continuous activation of the renin–angiotensin system (RAS) in renin-overexpressing hypertensive transgenic (Ren-Tg) mice. We treated 12-week-old male Ren-Tg and wild-type (WT) mice with a diet containing Riv (12 mg/kg/day) or a regular diet for 4 weeks. After this, FXa in plasma significantly increased in Ren-Tg mice compared with WT mice, and Riv inhibited this increase. Left ventricular wall thickness (LVWT) and the area of cardiac fibrosis evaluated by Masson's trichrome staining were greater in Ren-Tg mice than in WT mice, and Riv decreased them. Cardiac expression levels of the protease-activated receptor (PAR)-2, tumor necrosis factor-α, transforming growth factor (TGF)-β1, and collagen type 3 α1 (COL3A1) genes were all greater in Ren-Tg mice than in WT mice, and Riv attenuated these increases. To investigate the possible involvement of PAR-2, we treated Ren-Tg mice with a continuous subcutaneous infusion of 10 μg/kg/day of the PAR-2 antagonist FSLLRY for 4 weeks. FSLLRY significantly decreased LVWT and cardiac expression of PAR-2, TGF-β1, and COL3A1. In isolated cardiac fibroblasts (CFs), Riv or FSLLRY pretreatment inhibited the FXa-induced increase in the phosphorylation of extracellular signal-regulated kinases. In addition, Riv or FSLLRY inhibited FXa-stimulated wound closure in CFs. Riv exerts a protective effect against cardiac hypertrophy and fibrosis development induced by continuous activation of the RAS, partly by inhibiting PAR-2.

Keywords Factor Xa; · Rivaroxaban; · Cardiac hypertrophy; · Cardiac fibrosis; · Protease-activated receptor

Introduction

Heart failure (HF) is a serious health and economic issue worldwide and a major reason for hospitalization [1]. HF is caused by various types of heart diseases, such as hypertensive heart disease, cardiomyopathy, myocardial infarction (MI), valvular heart diseases, and congenital heart diseases [1]. The prognosis of HF patients is poor, even in those with a preserved ejection fraction (HFpEF) characterized by diastolic cardiac dysfunction [2, 3]. Continuous activation of the renin–angiotensin system (RAS) induces hypertensive organ damage, including cardiac hypertrophy, through enhanced afterload [4]. In addition, angiotensin (Ang) II, a main RAS effector, directly causes inflammation, endothelial dysfunction, and the generation of reactive oxygen species in the heart, independent of blood pressure, leading to HF [5]. Although RAS inhibition by angiotensin-converting enzyme inhibitors or Ang II receptor blockers is the most effective HF treatment [1], many HF patients suffer from repeated hospitalization and progressive symptoms and may be at risk of sudden cardiac death. More importantly, no treatment has been established for HFpEF [1].

✉ Hirofumi Tomita
tomitah@hirosaki-u.ac.jp

[1] Department of Cardiology and Nephrology, Hirosaki University Graduate School of Medicine, Hirosaki, Japan

[2] Department of Health Promotion, Hirosaki University Graduate School of Health Sciences, Hirosaki, Japan

[3] Division of Cardiology, Saiseikai Kumamoto Hospital Cardiovascular Center, Kumamoto, Japan

Accumulating evidence indicates the involvement of the coagulation pathway in RAS-induced cardiovascular remodeling [6–8]. For example, Ang II upregulates tissue factor (TF) expression in the plasma during hypertension, which leads to systemic activation of the coagulation cascade [6]. In addition, TF expression is upregulated in atherosclerotic plaques, and plaque rupture releases a large amount of TF [7, 8]. Factor Xa (FXa), an active form of factor X and one of the important components of the coagulation cascade, converts prothrombin into thrombin and accelerates thrombus formation [9]. In addition, FXa activates protease-activated receptor (PAR) and promotes inflammation by producing proinflammatory and profibrotic cytokines [10, 11]. PAR is distributed in many types of cells in the heart, including vascular endothelial cells, smooth muscle cells, cardiomyocytes, and cardiac fibroblasts (CFs) [10, 12], and is potentially associated with HF development [13, 14].

Direct oral anticoagulants are commonly used to prevent thromboembolic events, mainly those due to atrial fibrillation (AF) [15]. Rivaroxaban (Riv), a direct FXa inhibitor, acts as an anticoagulant by inhibiting FXa [16]. Although Riv exerts anti-inflammatory and anticoagulation effects [17, 18], the underlying mechanism is still unclear. In this study, we tested the hypothesis that Riv has a protective effect against HF progression induced by chronic RAS activation and evaluated the possible involvement of PAR-2 signaling in renin-overexpressing hypertensive transgenic (Ren-Tg) mice.

Methods

Animals and study protocols

We used Ren-Tg mice that overexpressed renin at a constant high level [19]. Briefly, a modified mouse renin transgene driven by a liver-specific albumin promoter/enhancer was inserted into the genome as a single copy at the liver-specific ApoA1/ApoC3 locus. The resulting transgene expressed renin ectopically at a constant high level in the liver, and high levels of active renin and Ang II in the plasma were observed. Ren-Tg mice display elevated systolic blood pressure (SBP) as early as 12 weeks old compared to wild-type (WT) mice [5, 19].

In this study, we used 12-week-old male heterozygous Ren-Tg and WT (C57BL6/N) mice. Ren-Tg mice were backcrossed with WT mice for >10 generations. Riv was supplied by Bayer Pharma AG (Berlin, Germany). We treated Ren-Tg and WT mice with either a diet containing Riv (12 mg/kg/day) or a regular diet for 4 weeks. SBP and pulse rate were measured and echocardiography was performed after this period. Then, the mice were anesthetized with one-time intraperitoneal injection of a mixture of 0.75 mg/kg medetomidine, 4 mg/kg midazolam, and 5 mg/kg butorphanol tartrate and were euthanized by cervical dislocation.

In the other experiments, we treated Ren-Tg mice with a continuous subcutaneous infusion of 10 μg/kg/day of the PAR-2 antagonist FSLLRY (Funakoshi, Tokyo, Japan) or saline (control) using an osmotic minipump (ALZET, Palo Alto, CA, USA) for 4 weeks. The procedure was performed under anesthesia as described above.

All procedures were performed in accordance with the Guide for the Care and Use of Laboratory Animals of the National Institutes of Health (NIH) and were approved by the Institutional Animal Care and Use Committee of Hirosaki University Graduate School of Medicine, Japan (approved number M14030).

FXa and active renin concentration in the plasma

FXa in the plasma was measured using a coagulation FXa ELISA Kit (MyBioSource, San Diego, CA, USA) according to the manufacturer's instructions. Briefly, after anesthesia with 3% isoflurane, blood was collected from the orbital venous plexus and stored on ice. Then, it was centrifuged at 1000 × *g* for 15 min at 4 °C, and the supernatant was collected as the plasma. Next, 100 μL of the plasma was added to each well of the coagulation FXa ELISA Kit, and 50 μL of conjugates was added and mixed. The kit was covered and incubated for 60 min at 37 °C, and analysis was done using Multiskan FC (Thermo Fisher Scientific, Waltham, MA, USA). The active renin concentration in the plasma was also measured by FRET-based assay kits (SensoLyte 520 Mouse Renin Assay kit; AnaSpec, Fremont, CA, USA). The effect of Riv on the active renin concentration was evaluated by adding a dose of 500 nM or 1 μM Riv to the assay.

Blood pressure and pulse rate measurements

Ren-Tg and WT mice were put in a warm chamber set at 37 °C for 10 min before measuring their SBP and pulse rate. SBP and pulse rate were measured by the tail-cuff method using BP-98A (Softron, Tokyo, Japan). After discarding the highest and lowest readings, at least 10 readings were averaged, as previously described [20].

Echocardiography

Echocardiography was performed using the HD11 XE with an L15-7io Broadband Compact Linear Array echocardiography system (Philips, Eindhoven, the Netherlands), and M-mode tracings were recorded from a short-axis view at the papillary muscle level, as previously described [5]. We

measured the left ventricular wall thickness (LVWT), calculated as interventricular septum thickness + posterior wall thickness, in diastole after treatment with or without Riv for 4 weeks. The values obtained from at least three cardiac cycles were averaged.

Quantitative polymerase chain reaction (PCR)

After euthanasia as described above, the hearts and aorta were rapidly excised, and the atria were removed and kept in liquid nitrogen. Small sections of the liver were also collected. Total RNA was isolated from the ventricles, aorta, and liver using the RNeasy Fibrous Tissue Mini Kit (Qiagen, Hilden, Germany) according to the manufacturer's instructions. Quantitative polymerase chain reaction (PCR) was performed using the CFX Connect™ Real-Time PCR Detection System (Bio-Rad, Hercules, CA, USA) with TaqMan Universal PCR Master Mix (Applied Biosystems, Foster City, CA, USA). Specific probes were obtained from Applied Biosystems to detect PAR-2 (Mm00433160_m1), tumor necrosis factor-alpha (TNF-α) (Mm0043258_m1), transforming growth factor-beta 1 (TGF-β1) (Mm01178820_m1), β-myosin heavy chain (β-MHC) (Mm00600532_g1), collagen type 3 α1 (COL3A1) (Mm01254476_m1), interleukin (IL)-1β (Mm00434228_m1), IL-6 (Mm0046190_m1), and glyceraldehyde-3-phosphate dehydrogenase (GAPDH) (Mm99999915_g1). Renin expression in the liver was examined as previously described [21]. The expression of each RNA was normalized to GAPDH.

Histological analysis

Ventricles were fixed in 10% formalin, embedded in paraffin, and stained with hematoxylin and eosin (H&E) or Masson's trichrome. Stained sections were visualized using a BZ-X710 fluorescence microscope (Keyence, Osaka, Japan) and analyzed using the BZ-X analyzer (Keyence).

Isolation of cardiac fibroblasts

We anesthetized 8–12-week-old WT mice with one-time intraperitoneal injection of a mixture of 0.75 mg/kg medetomidine, 4 mg/kg midazolam, and 5 mg/kg butorphanol tartrate and heparinized them by one-time intraperitoneal injection of heparin (200 U). The hearts were immediately excised, and the aortas were cannulated to the needle. The hearts were perfused with perfusion buffer containing 118 mM NaCl, 4.7 mM KCl, 1.2 mM $MgSO_4$, 1.2 mM KH_2PO_4, 25 mM $NaHCO_3$, 5.5 mM glucose, and 9.9 mM 2,3-butanedione 2-monoxime through a Langendorff apparatus (Physio-tech, Tokyo, Japan) set at 37 °C and a constant flow of 3 mL/min. After 3 min of perfusion, the buffer was changed to digestion buffer containing perfusion buffer plus 2 μM $CaCl_2$ and 0.24 U/mL Liberase TH Research grade (Sigma Aldrich, St. Louis, MO, USA), and perfusion continued for another 20 min. Then, the hearts were removed from the system, and the left ventricles were minced into small pieces. The mince was further digested in digestion buffer for an additional 10 min at 37 °C with gentle agitation and was filtered through a NITEX NYLON MESH with a 100 μm pore size (Genesee, San Diego, CA, USA). The mixture was centrifuged at 25 × *g* for 3 min to remove cardiomyocytes, and the supernatant was further centrifuged at 500 × *g* for 4 min to collect CFs. The CFs were grown in Dulbecco's modified Eagle medium supplemented with 10% fetal bovine serum (FBS), 10 U/mL penicillin, and 100 μg/mL streptomycin, and CFs at passage 2 were used for subsequent experiments.

Western blotting

CFs were plated on six-well dishes until reaching a confluence of 70–80%, serum-starved for 4 h, and pretreated with 0.3 μM Riv, 10 μM FSLLRY, or saline (control) for 30 min. Then, the CFs were stimulated with 20 nM FXa (Thermo Fisher Scientific, Waltham, MA, USA) for 30 min. After stimulation, the CFs were immediately lysed with RIPA lysis buffer (Santa Cruz Biotechnology, Santa Cruz, CA, USA) and centrifuged at 21,600 × *g* for 10 min. Protein concentrations were determined with the Protein Quantification Assay (MACHEREY-NAGEL GmbH & Co. KG, Duren, Germany). Proteins were separated by sodium dodecyl sulfide–polyacrylamide gel electrophoresis and electrophoretically transferred to polyvinylidene fluoride membranes (Bio-Rad, Hercules, CA, USA). After blocking with Blocking One-P (Nacalai Tesque, Kyoto, Japan) for phosphorylated extracellular signal-regulated kinase 1 and 2 (pERK) or 2% skim milk for total ERK (tERK), the membranes were incubated with primary antibody for pERK (Cell Signaling, Danvers, MA, USA) or tERK (Merck Millipore, MA, USA) overnight at 4 °C and then incubated with horseradish peroxidase goat anti–rabbit immunoglobulin G H&L secondary antibody (Abcam, Cambridge, UK) for 1 h at room temperature. Protein bands were visualized using Amersham ECL Prime Western Blotting Detection Reagents (GE Healthcare, Chicago, IL, USA), and densitometric analyses were performed in a ChemiDoc™ XRS+ with Image Lab™ Software (Bio-Rad).

Wound-healing assay

CFs were plated on six-well dishes at a confluence of 90–95% and kept in 0.1% FBS for 4 h. After pretreatment with 0.3 μM Riv, 10 μM FSLLRY, or saline (control) for 2.5 h, CFs were scraped off using a 200 μL sterile pipette tip (Labcon, Petaluma, CA, USA) and incubated with 20 nM

FXa for 48 h. The distance between one side of the wound and the other was measured at baseline and 48 h after the scratch. Digital photographs of each wound were taken using a Coolpix 950 camera (Nikon, Tokyo, Japan) and analyzed in ImageJ software (NIH). The wound closure percentage was calculated as (100 − [distance at initial scratch − distance at 48 h after scratch]/distance at initial scratch) × 100.

Statistical analysis

All data are expressed as mean ± standard deviation. Statistical significance was determined using the *t* test or one- or two-way analysis of variance (ANOVA) with Tukey's post hoc test in GraphPad Prism 8 software (GraphPad Software, San Diego, CA, USA). $P < 0.05$ was considered statistically significant.

Results

Riv inhibits increased FXa in Ren-Tg mice

To determine whether continuous RAS activation affects FXa and to evaluate the effect of Riv on FXa, we measured FXa in the plasma of Ren-Tg and WT mice with or without Riv. FXa in the plasma was significantly increased in Ren-Tg mice compared to WT mice (23.4 ± 2.6 vs. 13.3 ± 4.6 ng/mL; $P = 0.01$), and Riv significantly inhibited this increase to 11.4 ± 4.0 ng/mL in Ren-Tg mice ($P = 0.006$) (Fig. 1).

Blood pressure and pulse rate after 4 weeks of treatment

After 4 weeks of treatment, SBP was found to be significantly higher in Ren-Tg mice than in WT mice (130 ± 3 vs. 101 ± 4 mmHg, $P < 0.0001$), and Riv significantly decreased SBP to 119 ± 9 mmHg in Ren-Tg mice ($P = 0.01$). The pulse rate was found to be significantly higher in Ren-Tg mice than in WT mice (683 ± 21 vs. 600 ± 41 bpm, $P = 0.003$), and Riv had no effect on the pulse rate in Ren-Tg mice (696 ± 31 bpm, $P = 0.91$) (Table 1).

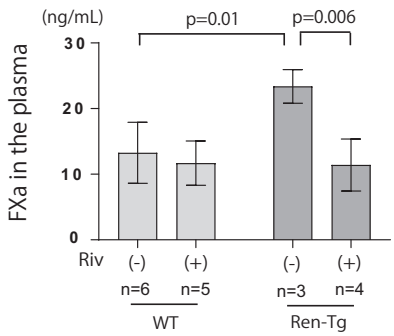

Fig. 1 Plasma FXa in Ren-Tg and WT mice after 4 weeks of treatment with or without Riv (n = 3–6). Comparisons were made by two-way ANOVA followed by Tukey's post hoc test. FXa indicates factor Xa, Ren-Tg renin-overexpressing hypertensive transgenic, WT wild-type, Riv rivaroxaban

Table 1 Systolic blood pressure and pulse rate in WT and Ren-Tg mice after 4 weeks of treatment

	WT mice		Ren-Tg mice	
Riv	−	+	−	+
SBP (mmHg)	101 ± 4	99 ± 3	130 ± 3*	119 ± 9†
Pulse rate (bpm)	600 ± 41	648 ± 45	683 ± 21**	696 ± 31

$n = 6$ in each group

WT wild type, *Ren-Tg* renin-overexpressing hypertensive, *Riv* rivaroxaban, *SBP* systolic blood pressure

*$p < 0.0001$ vs. WT without Riv, **$p = 0.003$ vs. WT without Riv, †$p = 0.01$ vs. Ren-Tg without Riv

Riv does not affect plasma active renin concentration or renin expression in the liver

To elucidate the underlying mechanism of the blood pressure-lowering effect of Riv in Ren-Tg mice, we measured the active renin concentration in the plasma. The active renin concentration was 1.54 ± 0.32-fold higher in Ren-Tg mice than in WT mice without Riv ($P = 0.04$, $n = 6$). Riv slightly lowered it by 0.75 ± 0.22-fold compared with its level in Ren-Tg mice without Riv, but this was not a significant difference ($P = 0.16$, $n = 6$). Pretreatment with 500 nM or 1 μM Riv had no effect on the active renin concentration in the plasma obtained from the Ren-Tg mice (1.00 ± 0.02-fold compared without Riv, $P = 0.98$ or 0.97 ± 0.05-fold, $P = 0.24$, respectively, $n = 5$–6).

Renin gene expression in the liver was detected in Ren-Tg mice, but not in WT mice. Riv did not affect its expression in the liver of Ren-Tg mice (0.89 ± 1.31-fold compared with Ren-Tg mice without Riv, $P = 0.85$, $n = 6$).

Riv attenuates cardiac hypertrophy and fibrosis in Ren-Tg mice

Our previous study and another report showed that Ren-Tg mice display cardiac hypertrophy and fibrosis as early as 12 weeks old, unlike WT mice [5, 22]. To determine whether Riv treatment attenuates cardiac hypertrophy and fibrosis, we fed Ren-Tg and WT mice a diet with or without Riv and evaluated its effects. Figure 2A shows representative cross-sections of ventricles stained with H&E in Ren-Tg and WT mice fed a diet with or without Riv for 4 weeks. LVWT was significantly higher in Ren-Tg mice than in WT mice (2.2 ± 0.1 vs. 1.8 ± 0.1 mm; $P < 0.0001$), and Riv

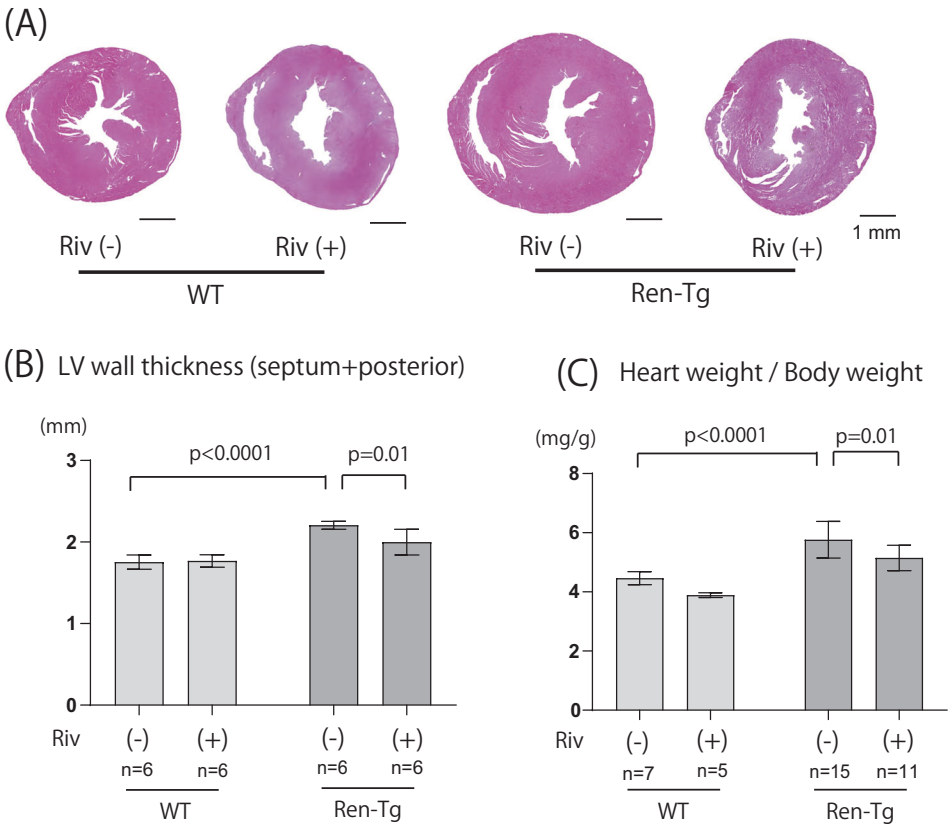

Fig. 2 Effects of Riv on cardiac hypertrophy and heart weight in Ren-Tg and WT mice. **A** Representative images (×25) of hearts stained with hematoxylin and eosin in Ren-Tg and WT mice after 4 weeks of treatment with or without Riv. **B** The LV wall thickness (interventricular septum + posterior wall thickness) in Ren-Tg and WT mice treated with or without Riv, evaluated by echocardiography ($n = 6$). Comparisons were made by two-way ANOVA followed by Tukey's post hoc test. **C** Heart weight:body weight ratio in Ren-Tg and WT mice after 4 weeks of treatment with or without Riv ($n = 5$–15). Comparisons were made by two-way ANOVA followed by Tukey's post hoc test. Ren-Tg indicates renin-overexpressing hypertensive transgenic, WT wild-type, Riv rivaroxaban, LV left ventricular

significantly attenuated the increase to 2.0 ± 0.2 mm in Ren-Tg mice ($P = 0.01$) (Fig. 2B).

Morphological analysis showed that the heart weight (HW):body weight (BW) ratio was higher in Ren-Tg mice than in WT mice (5.8 ± 0.6 vs. 4.5 ± 0.2 mg/g; $P < 0.0001$), and Riv attenuated the increase to 5.1 ± 0.4 mg/g in Ren-Tg mice ($P = 0.01$) (Fig. 2C). Representative sections of ventricles stained with Masson's trichrome from Ren-Tg and WT mice treated with or without Riv for 4 weeks are shown in Fig. 3A. The area of cardiac interstitial fibrosis was significantly greater in Ren-Tg mice than in WT mice (4.2 ± 0.7 vs. 1.1 ± 0.6%; $P < 0.0001$), and Riv reduced the area to 2.2 ± 1.1% in Ren-Tg mice ($P = 0.0005$) (Fig. 3B). These findings indicate that continuous RAS activation causes cardiac hypertrophy and fibrosis and that Riv attenuates these effects.

Riv attenuates the increase in proinflammatory and profibrotic cytokines

To investigate the mechanism underlying the protective effects of Riv against cardiac hypertrophy and fibrosis, we measured cardiac gene expression related to proinflammatory and profibrotic processes in the heart. PAR-2, TNF-α, TGF-β1, β-MHC, and COL3A1 expression in Ren-Tg mice was higher than that in WT mice ($P = 0.03$, $P = 0.03$, $P = 0.02$, $P < 0.0001$, and $P = 0.049$, respectively). Riv significantly inhibited the increases in PAR-2 ($P = 0.04$), TNF-α ($P = 0.003$), TGF-β1 ($P = 0.004$), β-MHC ($P = 0.01$), and COL3A1 ($P = 0.03$) expression in Ren-Tg mice (Fig. 4A–E). These results indicate that continuous RAS activation causes upregulation of PAR-2 and production of proinflammatory and profibrotic cytokines and thereby contributes to cardiac hypertrophy and fibrosis development. Riv inhibits cardiac hypertrophy and fibrosis, and attenuates the production of these cytokines.

FSLLRY attenuates cardiac hypertrophy and the increase in proinflammatory and profibrotic cytokines

FXa activates PAR-2 and promotes inflammatory and fibrotic processes [23, 24]. To investigate the involvement of PAR-2 signaling in RAS-induced cardiac remodeling, we treated Ren-Tg mice with a continuous subcutaneous injection of the PAR-2 antagonist FSLLRY for 4 weeks and evaluated its effects. The LVWT in the FSLLRY group was significantly lower than that in the controls (2.0 ± 0.2 vs. 2.4 ± 0.2 mm; $P = 0.04$) (Fig. 5A). In addition, 4 weeks of FSLLRY treatment significantly decreased the HW–BW ratio compared to the control (6.5 ± 0.2 vs. 6.0 ± 0.4 mg/g; $P = 0.03$) (Fig. 5B). SBP was significantly lower in Ren-Tg mice after FSLLRY treatment for 4 weeks than in those

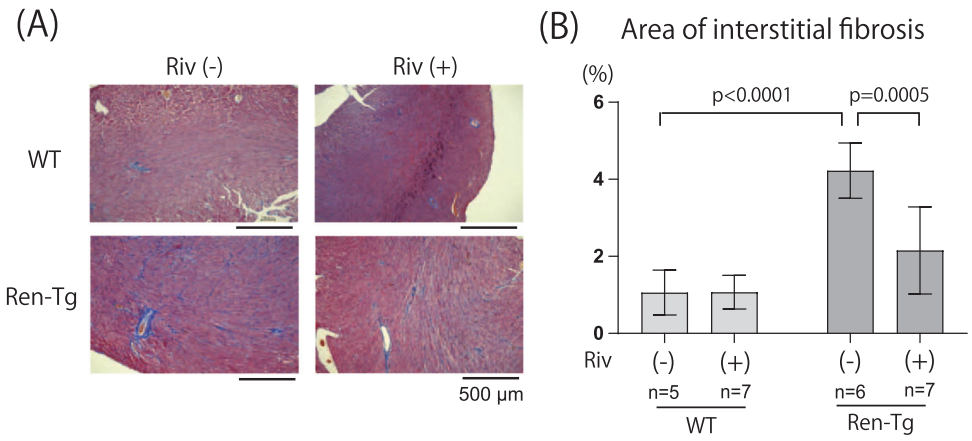

Fig. 3 Assessment of cardiac interstitial fibrosis after 4 weeks of treatment with or without Riv in Ren-Tg and WT mice. **A** Representative images (×100) of hearts stained with Masson's trichrome. **B** Evaluation of the interstitial fibrosis area ($n =$ 5–7). Comparisons were made by two-way ANOVA followed by Tukey's post hoc test. Ren-Tg indicates renin-overexpressing hypertensive transgenic, WT wild-type, Riv rivaroxaban

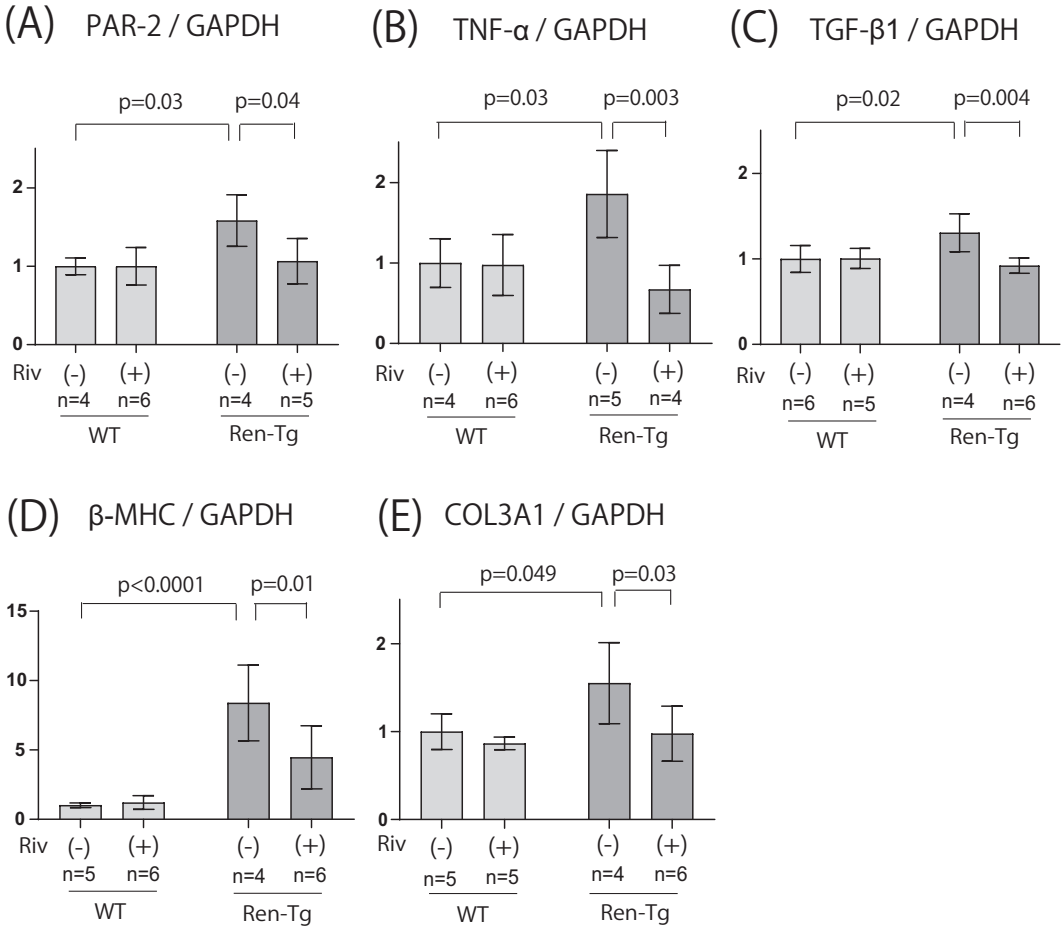

Fig. 4 Effects of Riv on the gene expression of PAR-2 and proinflammatory and profibrotic cytokines in the heart. Gene expression of PAR-2 (**A**), TNF-α (**B**), TGF-β1 (**C**), β-MHC (**D**), and COL3A1 (**E**) in Ren-Tg and WT mice ($n = 4$–6). Comparisons were made by two-way ANOVA followed by Tukey's post hoc test. Ren-Tg indicates renin-overexpressing hypertensive transgenic, WT wild-type, Riv rivaroxaban, PAR-2 protease-activated receptor-2, TNF-α tumor necrosis factor-α, TGF-β1 transforming growth factor-β1, β-MHC β-myosin heavy chain, COL3A1 collagen type 3 α1, GAPDH glyceraldehyde-3-phosphate dehydrogenase

without it (115 ± 2 vs. 134 ± 3 mmHg, $P < 0.0001$, $n = 4$ in each group).

PAR-2 gene expression in the hearts of Ren-Tg mice was lower in the FSLLRY group than in the controls ($P = 0.004$) (Fig. 6A). Similarly, TGF-β1, β-MHC, and COL3A1 gene expression was significantly lower in the FSLLRY group than in the controls ($P = 0.04$, $P = 0.02$, and $P = 0.04$, respectively) (Fig. 6C–E). A similar trend

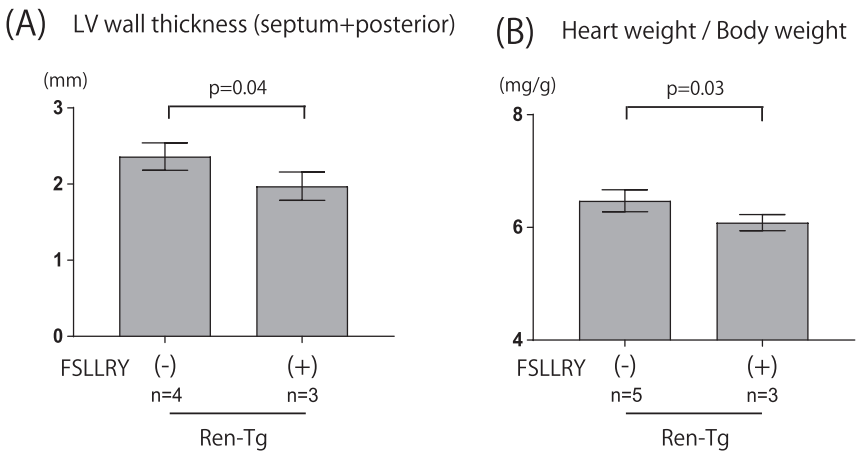

Fig. 5 Effects of the PAR-2 antagonist FSLLRY on cardiac hypertrophy and heart weight in Ren-Tg mice. **A** LV wall thickness (interventricular septum + posterior wall thickness) in Ren-Tg mice treated with or without FSLLRY, evaluated by echocardiography ($n = 3$–4). Comparisons were made by unpaired Student's t test. **B** Heart weight:body weight ratio in Ren-Tg mice after 4 weeks of treatment with or without FSLLRY ($n = 3$–5). Comparisons were made by unpaired Student's t test. Ren-Tg indicates renin-overexpressing hypertensive transgenic, PAR-2 protease-activated receptor-2, LV left ventricular

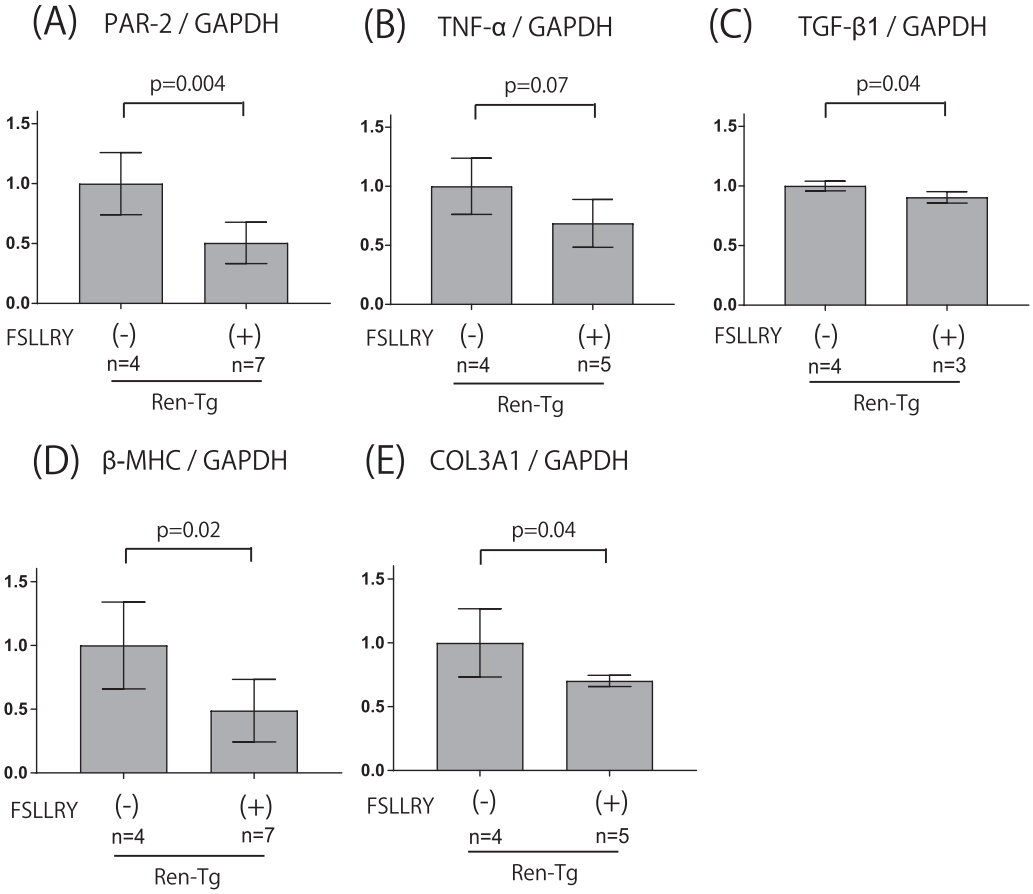

Fig. 6 Effects of the PAR-2 antagonist FSLLRY on cardiac gene expression in Ren-Tg mice. Gene expression of PAR-2 (**A**), TNF-α (**B**), TGF-β1 (**C**), β-MHC (**D**), and COL3A1 (**E**) in Ren-Tg mice ($n = 3$–7). Comparisons were made by unpaired student's t test. PAR-2 indicates protease-activated receptor-2, Ren-Tg renin-overexpressing hypertensive transgenic, TGF-β1 transforming growth factor-β1, β-MHC β-myosin heavy chain, COL3A1 collagen type 3 α1, GAPDH glyceraldehyde-3-phosphate dehydrogenase

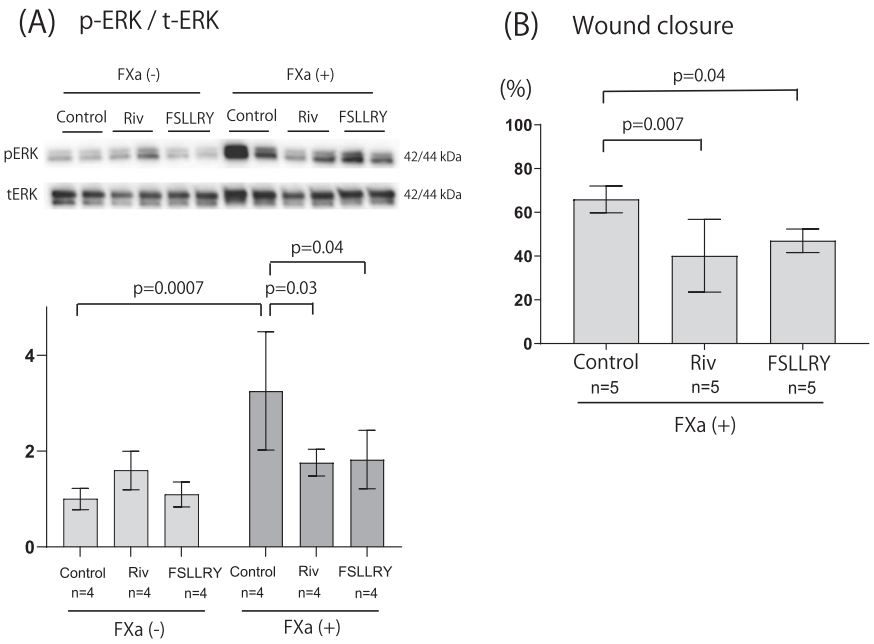

Fig. 7 **A** Ratio of pERK to tERK after stimulation by 20 nM FXa for 30 min in isolated CFs treated with either 0.3 μM Riv or 10 μM of the PAR-2 antagonist FSLLRY ($n = 4$). Representative images of western blotting are shown. Comparisons were made by two-way ANOVA followed by Tukey's post hoc test. **B** Wound-healing assay in isolated CFs treated with either 0.3 μM Riv or 10 μM FSLLRY ($n = 5$). Comparisons were made by one-way ANOVA followed by Tukey's post hoc test. pERK indicates phosphorylated extracellular signal-regulated kinase 1 and 2, tERK total extracellular signal-regulated kinase 1 and 2, FXa factor Xa, Riv rivaroxaban, CFs cardiac fibroblasts, PAR-2 protease-activated receptor-2

was found in TNF-α gene expression, although the difference was not statistically significant ($P = 0.07$) (Fig. 6B). These results indicate that FSLLRY attenuates cardiac hypertrophy and contributes to inhibiting the production of proinflammatory and profibrotic cytokines in the heart.

Riv or FSLLRY inhibits ERK1/2 phosphorylation and wound healing in CFs

CFs play a central role in the production of the extracellular matrix (ECM) and interstitial fibrosis in the heart [25]. To further evaluate the inhibitory effect of Riv and FSLLRY on cardiac hypertrophy and fibrosis, we examined mitogen-activated protein kinase (MAPK) signaling in isolated CFs. ERK phosphorylation was significantly increased in response to FXa ($P = 0.0007$ vs. controls), and Riv or FSLLRY pretreatment significantly inhibited ERK phosphorylation ($P = 0.03$ and $P = 0.04$ vs. controls, respectively) (Fig. 7A). Next, we evaluated the effects of Riv or FSLLRY on CF migration and proliferation using a wound-healing assay. Riv or FSLLRY significantly inhibited wound closure in response to FXa ($P = 0.007$ and $P = 0.04$ vs. controls, respectively) (Fig. 7B), indicating that Riv and FSLLRY inhibit CF migration and proliferation. These results indicate that FXa induces MAPK activation and CF migration and proliferation, presumably via PAR-2 signaling, potentially leading to cardiac interstitial fibrosis.

Riv inhibits the increase in IL-1β and TNF-α expression in the aorta

We next evaluated vascular inflammation induced by continuous activation of the RAS. The levels of IL-1β and TNF-α in the aorta were significantly increased in Ren-Tg mice compared with WT mice ($P = 0.048$ and $P = 0.03$, respectively), and Riv attenuated the increase in IL-1β ($P = 0.03$) and TNF-α gene expression ($P = 0.047$) (Fig. 8A, B). Although a similar trend was found in IL-6 expression, it was not significant (Fig. 8C). These results indicate that Riv inhibits vascular inflammation, which may ameliorate the progression of vascular remodeling and may be one of the mechanisms of the blood pressure-lowering effect of Riv.

Discussion

The major findings of the present study are as follows: (1) FXa in the plasma was increased in Ren-Tg mice compared to WT mice and was inhibited by Riv, (2) Riv attenuated cardiac hypertrophy and fibrosis progression by inhibiting proinflammatory and profibrotic cytokine production in Ren-Tg mice, (3) the PAR-2 antagonist FSLLRY

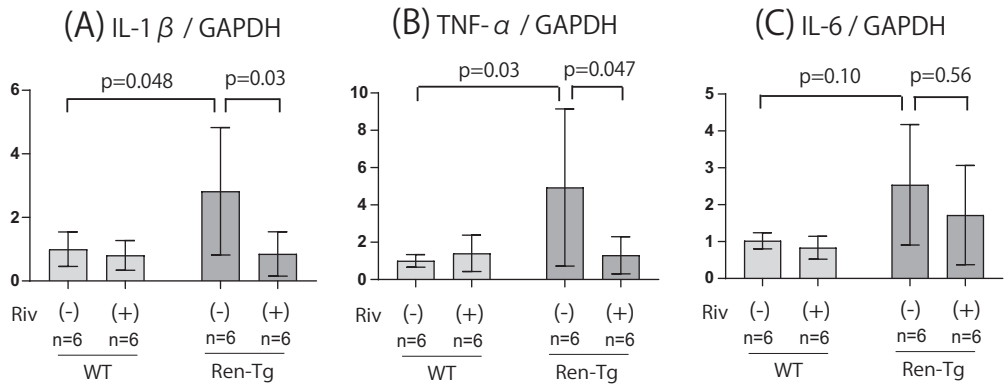

Fig. 8 Effects of Riv on the gene expression of IL-1β (**A**), TNF-α (**B**), and IL-6 (**C**) in the aorta of Ren-Tg and WT mice after 4 weeks of treatment with or without Riv ($n = 6$). Comparisons were made by two-way ANOVA followed by Tukey's post hoc test. Ren-Tg indicates renin-overexpressing hypertensive transgenic, WT wild-type, Riv rivaroxaban, IL-1β interleukin-1β, TNF-α tumor necrosis factor-α, IL-6 interleukin-6, GAPDH glyceraldehyde-3-phosphate dehydrogenase

attenuated cardiac hypertrophy and proinflammatory and profibrotic cytokine production in Ren-Tg mice, and (4) Riv or FSLLRY inhibited ERK phosphorylation and CF proliferation and migration in response to FXa. These findings indicate that Riv might have protective effects against cardiac hypertrophy and fibrosis development caused by chronic activation of RAS, partly through inhibition of PAR-2 signaling.

RAS activation causes vasoconstriction and enhanced sodium reabsorption in renal tubules, resulting in SBP elevation and fluid retention [4, 5, 26]. Regulation of RAS activity plays an important role in maintaining systemic hemodynamics; however, chronic activation of RAS directly and indirectly causes damage to organs, including the heart [27]. In this study, we used Ren-Tg mice to focus on the role of the RAS in HF development, because RAS activation is commonly observed in HF patients [28] and RAS inhibition is a standard pharmacological treatment [1]. Riv attenuated cardiac hypertrophy and fibrosis induced by chronic RAS activation by inhibiting the production of proinflammatory and profibrotic cytokines. Riv functions as an anticoagulant by inhibiting FXa, so we measured FXa in the plasma. We found that continuous activation of RAS upregulated FXa, and Riv inhibited the increase in plasma FXa in Ren-Tg mice. Recently, Hara et al. reported that plasma FXa level is positively correlated with the severity of coronary artery disease [29]. In addition, we recently showed that Riv-induced FXa inhibition attenuates hypertensive renal damage [20]. Therefore, FXa may be a key molecule to promote cardiovascular remodeling induced by chronic RAS activation, and our findings may provide important clinical implications to improve our understanding of HF pathogenesis in patients who have hypertension as a coexisting condition. A possible mechanism for the inhibitory effect of Riv on plasma FXa concentration is of interest. The expression of TF is upregulated by Ang II in endothelial cells and vascular smooth muscle cells [30, 31]. TF is also upregulated in hypertensive rats throughout the endothelium and media of blood vessels, and blocking the Ang II type 1 receptor (AT1R) inhibits the upregulation of TF expression [32]. Although we did not measure TF expression in the present study, the increase in TF expression by RAS activation seems to yield an increase in FXa and thereby activate PAR-2 signaling. Importantly, PAR-2 signaling, not PAR-1, activates TF signaling via phosphorylation of the TF cytoplasmic domain [33] and further accelerates the coagulation cascade. Taken together, the evidence suggests Riv might reduce the activity of the TF-mediated coagulation cascade, including FXa, partly by inhibiting PAR-2 signaling and consequently decrease the plasma FXa concentration in Ren-Tg mice. In fact, administration of a PAR-1 antagonist did not reduce the plasma FXa concentration in Ren-Tg mice in our previous study [34].

FXa activates PAR-2 and initiates proinflammatory and profibrotic processes, including MAPK signaling [10]. PAR-2 is expressed in a variety of cells in the heart, including vascular endothelial cells, smooth muscle cells, cardiomyocytes, and fibroblasts [11, 12, 35], and plays an important role in cardiac remodeling induced by various stimuli [36–38]. Specifically, FXa-induced ERK phosphorylation, proliferation, and differentiation into myofibroblasts are mediated through PAR-2 signaling in fibroblasts [39]. Ang II-induced ECM and proinflammatory and profibrotic cytokine production are inhibited by FSLLRY in adventitial fibroblasts [38]. In addition, Riv protects against cardiac dysfunction development in an MI model, which is diminished by PAR-2 knockout [13]. All these findings indicate that PAR-2 signaling promotes inflammatory and fibrotic processes and contributes to HF development. In this study, we focused on PAR-2 signaling as a target of FXa and its potential role in HF development

induced by chronic RAS activation. We found that PAR-2 expression in the heart was increased in Ren-Tg mice compared to WT mice, and Riv or FSLLRY inhibited this increase. In addition, FSLLRY attenuated the progression of cardiac hypertrophy and proinflammatory and profibrotic cytokine production in Ren-Tg mice. These results indicate that upregulation of FXa by chronic RAS activation causes cardiac hypertrophy and fibrosis partly through PAR-2 signaling.

Downregulation in response to continuous excessive agonist stimulation in the heart is a well-known response of β-adrenergic receptor (β-AR) and AT1R, which comes about by translocation of the receptors from the cell membrane into the cytosol followed by degradation of the receptor in lysosomes [40]. In contrast, PAR-1 and PAR-2 expression is reported to be increased in the ischemic heart [41], and PAR-2 expression is increased in the pressure-overloaded heart [42]. Moreover, our previous studies demonstrated that PAR-2 expression is enhanced in the kidney [20] and that PAR-1 expression is also enhanced in the heart concomitantly with increased TNF-α and TGF-β1 expression in Ren-Tg mice [34]. Importantly, the PAR-1 antagonist SCH79797 decreases PAR-1 expression in the heart and in isolated CFs concomitantly with attenuated TNF-α and TGF-β1 upregulation. These results indicate that PAR expression seems to be regulated by different mechanisms than β-AR or AT1R. Previous reports demonstrated that PAR expression is positively regulated by inflammatory cytokines such as TNF-α and IL-1β in various types of cells [43–45]. These findings and our results may indicate that enhancement of inflammatory cytokines upregulates PAR-2 expression in the heart, and Riv or FSLLRY inhibits the expression of the inflammatory cytokines, resulting in decreased PAR-2 expression.

To further elucidate the mechanism underlying cardiac hypertrophy and fibrosis development induced by chronic RAS activation and the possible involvement of PAR-2 signaling, we next examined the role of CFs. CFs are the largest population of interstitial cells in the heart and are responsible for producing the ECM [25]. Recent studies using novel tissue-specific conditional knockout technology have demonstrated that CFs function as regulators of not only ECM production but also cardiac hypertrophy and systolic function [46]. In this study, FXa significantly enhanced ERK phosphorylation in CFs, and Riv or FSLLRY blocked it. In addition, Riv or FSLLRY inhibited wound healing stimulated by FXa. As ERK activation is closely associated with ECM production and tissue fibrosis [47, 48], our results indicate that FXa upregulation by chronic RAS activation induces MAPK activation and CF migration and proliferation, resulting in cardiac fibrosis partly via PAR-2 signaling.

In terms of vascular physiology, intravenous administration of FXa or PAR-2 agonist elicits a dose-dependent relaxation of the artery and decreases SBP via a nitric oxide (NO)-dependent mechanism [49, 50]. PAR-2-induced vasodilation is preserved in metabolic syndrome or diabetic models even though NO-mediated vasodilation is attenuated [51, 52]. In our study, SBP was not affected by Riv in WT mice, indicating that FXa is not part of the regulation of SBP under normal conditions. In contrast, Riv and FSLLRY modestly but significantly decreased SBP in Ren-Tg mice. To elucidate the underlying mechanisms of the blood pressure-lowering effect of Riv, we studied vascular inflammation in Ren-Tg mice and the effects of Riv on it. We found that the gene expression of inflammatory cytokines such as IL-1β and TNF-α in the aorta of Ren-Tg mice was enhanced and that Riv attenuated these increases. A recent study showed that Riv attenuates atherosclerotic plaque progression in apolipoprotein E (apoE)-deficient mice [53] and endothelial dysfunction in a diabetic model [54]. Furthermore, FXa inhibition limits the development of aortic aneurysm and the progression of atherosclerosis in Ang II-infused apoE-deficient mice [55]. More strikingly, PAR-2 deficiency attenuates the progression of atherosclerosis in apoE-deficient mice while reducing the expression of inflammatory cytokines such as TNF-α [56]. It should be noted that Riv did not affect renin expression in the liver or plasma active renin concentration in Ren-Tg mice in the present study. This is supported by a previous report showing that Riv is highly selective for FXa, more than 10,000-fold higher than for other serine proteases, such as factor VIIa, factor IXa, factor XIa, thrombin, activated protein C, plasmin, urokinase, and trypsin [16]. These findings and our results indicate that Riv inhibits vascular inflammation caused by RAS, which may attenuate the increase in vascular resistance and may consequently lower SBP in Ren-Tg mice.

It is of interest to determine whether inhibition of cardiac hypertrophy in Ren-Tg mice by Riv and FSLLRY is caused by PAR-2 inhibition or SBP-lowering effects. Ang II acts as a strong vasoconstrictor and promotes hypertrophic and fibrotic responses in the heart by enhancing afterload. In addition, Ang II directly affects the heart via AT1R and enhances the inflammatory process, which accelerates cardiac remodeling independent of blood pressure [57]. In fact, cardiac remodeling induced by Ang II infusion is markedly exacerbated in mice overexpressing C-reactive protein partly through upregulation of TNF-α and TGF-β1 without affecting blood pressure [58]. Other reports also support the direct effect of Ang II on the heart, independent of increased afterload [42, 59]. Furthermore, our previous study demonstrated that lowering blood pressure by hydralazine does not attenuate cardiac hypertrophy and fibrosis in Ren-Tg mice [5], indicating that cardiac hypertrophy in Ren-Tg

mice cannot be inhibited by only lowering blood pressure. In the present study, the expression of TNF-α and TGF-β1 in the heart was enhanced in Ren-Tg mice, and Riv treatment attenuated these increases. Furthermore, Riv or FSLLRY inhibited FXa-induced ERK phosphorylation and wound closure in isolated CFs. Although it may be difficult to completely separate the cardiac effect of Ang II from its hemodynamic action, our results indicate that Riv may inhibit the progression of cardiac hypertrophy and fibrosis at least in part by inhibiting PAR-2 signaling.

In the clinical setting, FXa inhibitors, including Riv, have been widely used for the prevention of stroke or systemic thromboembolism in patients with nonvalvular AF (NVAF). In the ROCKET AF (An Efficacy and Safety Study of Rivaroxaban With Warfarin for the Prevention of Stroke and Non–Central Nervous System Systemic Embolism in Patients With Nonvalvular Atrial Fibrillation) study, Riv was shown to be noninferior to warfarin in preventing stroke or systemic thromboembolism [15]. Notably, 90% of the patients in that clinical trial had hypertension as a coexisting condition [15]. Since hypertension is known to be one of the most important risk factors for the incidence of HFpEF [60], our results raise the possibility that Riv may be useful for the prevention of HFpEF and its treatment in patients with NVAF. Further clinical studies are clearly required.

In conclusion, Riv attenuates cardiac hypertrophy and fibrosis induced by chronic RAS activation, partly by inhibiting PAR-2 signaling. Riv-induced FXa inhibition might be a new therapeutic strategy for HF induced by chronic RAS activation.

Acknowledgements We thank Nahomi Miyamoto, Ritsuko Kasai, and Chuya Murakami for their excellent technical support.

Funding This work was partially supported by Bayer Yakuhin, Ltd., Japan.

Compliance with ethical standards

Conflict of interest HT received a scholarship or donation from Boehringer Ingelheim, Bayer, Daiichi-Sankyo, and Pfizer and speakers' bureau/honorarium agreements from Boehringer Ingelheim, Bayer, and Daiichi-Sankyo. KO received speakers' bureau/honorarium agreements from Daiichi-Sankyo, Boehringer Ingelheim, and Bayer. The remaining authors have no disclosures to report.

Publisher's note Springer Nature remains neutral with regard to jurisdictional claims in published maps and institutional affiliations.

References

1. Yancy CW, Jessup M, Bozkurt B, Butler J, Casey DE Jr., Colvin MM, et al. 2017 ACC/AHA/HFSA focused update of the 2013 ACCF/AHA guideline for the management of heart failure: a report of the American College of Cardiology/American Heart Association task force on clinical practice guidelines and the Heart Failure Society of America. J Am Coll Cardiol. 2017;70:776–803.
2. Mosterd A, Cost B, Hoes AW, de Bruijne MC, Deckers JW, Hofman A, et al. The prognosis of heart failure in the general population: the Rotterdam Study. Eur Heart J. 2001;22:1318–27.
3. Vasan RS, Larson MG, Benjamin EJ, Evans JC, Reiss CK, Levy D. Congestive heart failure in subjects with normal versus reduced left ventricular ejection fraction: prevalence and mortality in a population-based cohort. J Am Coll Cardiol. 1999;33:1948–55.
4. Mehta PK, Griendling KK. Angiotensin II cell signaling: physiological and pathological effects in the cardiovascular system. Am J Physiol Cell Physiol. 2007;292:C82–97.
5. Tanno T, Tomita H, Narita I, Kinjo T, Nishizaki K, Ichikawa H, et al. Olmesartan inhibits cardiac hypertrophy in mice overexpressing renin independently of blood pressure: its beneficial effects on ACE2/Ang(1-7)/Mas axis and NADPH oxidase expression. J Cardiovasc Pharmacol. 2016;67:503–9.
6. Antoniak S, Sparkenbaugh E, Pawlinski R. Tissue factor, protease activated receptors and pathologic heart remodelling. Thromb Haemost. 2014;112:893–900.
7. Steffel J, Luscher TF, Tanner FC. Tissue factor in cardiovascular diseases: molecular mechanisms and clinical implications. Circulation. 2006;113:722–31.
8. Tatsumi K, Mackman N. Tissue factor and atherothrombosis. J Atheroscler Thromb. 2015;22:543–9.
9. Esmon CT. Targeting factor Xa and thrombin: impact on coagulation and beyond. Thromb Haemost. 2014;111:625–33.
10. Hirano K. The roles of proteinase-activated receptors in the vascular physiology and pathophysiology. Arterioscler Thromb Vasc Biol. 2007;27:27–36.
11. Steinberg SF. The cardiovascular actions of protease-activated receptors. Mol Pharmacol. 2005;67:2–11.
12. McLarty JL, Melendez GC, Brower GL, Janicki JS, Levick SP. Tryptase/Protease-activated receptor 2 interactions induce selective mitogen-activated protein kinase signaling and collagen synthesis by cardiac fibroblasts. Hypertension. 2011;58:264–70.
13. Bode MF, Auriemma AC, Grover SP, Hisada Y, Rennie A, Bode WD, et al. The factor Xa inhibitor rivaroxaban reduces cardiac dysfunction in a mouse model of myocardial infarction. Thromb Res. 2018;167:128–34.
14. Pawlinski R, Tencati M, Hampton CR, Shishido T, Bullard TA, Casey LM, et al. Protease-activated receptor-1 contributes to cardiac remodeling and hypertrophy. Circulation. 2007;116:2298–306.
15. Patel MR, Mahaffey KW, Garg J, Pan G, Singer DE, Hacke W, et al. Rivaroxaban versus warfarin in nonvalvular atrial fibrillation. N Engl J Med. 2011;365:883–91.
16. Perzborn E, Strassburger J, Wilmen A, Pohlmann J, Roehrig S, Schlemmer KH, et al. In vitro and in vivo studies of the novel antithrombotic agent BAY 59-7939–an oral, direct Factor Xa inhibitor. J Thromb Haemost. 2005;3:514–21.
17. Zhou Q, Bea F, Preusch M, Wang H, Isermann B, Shahzad K, et al. Evaluation of plaque stability of advanced atherosclerotic lesions in apo E-deficient mice after treatment with the oral factor Xa inhibitor rivaroxaban. Mediators Inflamm. 2011;2011:432080.
18. Hashikata T, Yamaoka-Tojo M, Namba S, Kitasato L, Kameda R, Murakami M, et al. Rivaroxaban inhibits angiotensin II-induced activation in cultured mouse cardiac fibroblasts through the modulation of NF-kappaB pathway. Int Heart J. 2015;56:544–50.
19. Caron KM, James LR, Kim HS, Morham SG, Sequeira Lopez ML, Gomez RA, et al. A genetically clamped renin transgene for the induction of hypertension. Proc Natl Acad Sci USA. 2002;99:8248–52.
20. Ichikawa H, Shimada M, Narita M, Narita I, Kimura Y, Tanaka M, et al. Rivaroxaban, a direct factor Xa inhibitor, ameliorates hypertensive renal damage through inhibition of the inflammatory

response mediated by protease-activated receptor pathway. J Am Heart Assoc. 2019;8:e012195.
21. Caron KM, James LR, Lee G, Kim HS, Smithies O. Lifelong genetic minipumps. Physiol Genom. 2005;20:203–9.
22. Caron KM, James LR, Kim HS, Knowles J, Uhlir R, Mao L, et al. Cardiac hypertrophy and sudden death in mice with a genetically clamped renin transgene. Proc Natl Acad Sci USA. 2004;101: 3106–11.
23. Antoniak S, Sparkenbaugh EM, Tencati M, Rojas M, Mackman N, Pawlinski R. Protease activated receptor-2 contributes to heart failure. PLoS ONE. 2013;8:e81733.
24. Sabri A, Muske G, Zhang H, Pak E, Darrow A, Andrade-Gordon P, et al. Signaling properties and functions of two distinct cardiomyocyte protease-activated receptors. Circ Res. 2000;86:1054–61.
25. Brown RD, Ambler SK, Mitchell MD, Long CS. The cardiac fibroblast: therapeutic target in myocardial remodeling and failure. Annu Rev Pharmacol Toxicol. 2005;45:657–87.
26. Patel S, Rauf A, Khan H, Abu-Izneid T. Renin-angiotensin-aldosterone (RAAS): The ubiquitous system for homeostasis and pathologies. Biomed Pharmacother. 2017;94:317–25.
27. Duprez DA. Role of the renin-angiotensin-aldosterone system in vascular remodeling and inflammation: a clinical review. J Hypertens. 2006;24:983–91.
28. Ueda T, Kawakami R, Nishida T, Onoue K, Soeda T, Okayama S, et al. Plasma renin activity is a strong and independent prognostic indicator in patients with acute decompensated heart failure treated with renin-angiotensin system inhibitors. Circ J. 2015;79:1307–14.
29. Hara T, Phuong PT, Fukuda D, Yamaguchi K, Murata C, Nishimoto S, et al. Protease-activated receptor-2 plays a critical role in vascular inflammation and atherosclerosis in apolipoprotein E-deficient mice. Circulation. 2018;138:1706–19.
30. Sugano T, Tsuji H, Masuda H, Nishimura H, Yoshizumi M, Kawano H, et al. Adrenomedullin inhibits angiotensin II-induced expression of tissue factor and plasminogen activator inhibitor-1 in cultured rat aortic endothelial cells. Arterioscler Thromb Vasc Biol. 2001;21:1078–83.
31. Taubman MB, Marmur JD, Rosenfield CL, Guha A, Nichtberger S, Nemerson Y. Agonist-mediated tissue factor expression in cultured vascular smooth muscle cells. Role of Ca^{2+} mobilization and protein kinase C activation. J Clin Investig. 1993;91:547–52.
32. Müller DN, Mervaala EM, Dechend R, Fiebeler A, Park JK, Schmidt F, et al. Angiotensin II (AT(1)) receptor blockade reduces vascular tissue factor in angiotensin II-induced cardiac vasculopathy. Am J Pathol. 2000;157:111–22.
33. Ahamed J, Ruf W. Protease-activated receptor 2-dependent phosphorylation of the tissue factor cytoplasmic domain. J Biol Chem. 2004;279:23038–44.
34. Yokono Y, Hanada K, Narita M, Tatara Y, Kawamura Y, Miura N, et al. Blockade of PAR-1 signaling attenuates cardiac hypertrophy and fibrosis in renin-overexpressing hypertensive mice. J Am Heart Assoc. 2020;9:e015616.
35. Sabri A, Short J, Guo J, Steinberg SF. Protease-activated receptor-1-mediated DNA synthesis in cardiac fibroblast is via epidermal growth factor receptor transactivation: distinct PAR-1 signaling pathways in cardiac fibroblasts and cardiomyocytes. Circ Res. 2002;91:532–9.
36. Snead AN, Insel PA. Defining the cellular repertoire of GPCRs identifies a profibrotic role for the most highly expressed receptor, protease-activated receptor 1, in cardiac fibroblasts. FASEB J. 2012;26:4540–7.
37. Borensztajn K, Bresser P, van der Loos C, Bot I, van den Blink B, den Bakker MA, et al. Protease-activated receptor-2 induces myofibroblast differentiation and tissue factor up-regulation during bleomycin-induced lung injury: potential role in pulmonary fibrosis. Am J Pathol. 2010;177:2753–64.
38. He RQ, Tang XF, Zhang BL, Li XD, Hong MN, Chen QZ, et al. Protease-activated receptor 1 and 2 contribute to angiotensin II-induced activation of adventitial fibroblasts from rat aorta. Biochem Biophys Res Commun. 2016;473:517–23.
39. Borensztajn K, Stiekema J, Nijmeijer S, Reitsma PH, Peppelenbosch MP, Spek CA. Factor Xa stimulates proinflammatory and profibrotic responses in fibroblasts via protease-activated receptor-2 activation. Am J Pathol. 2008;172:309–20.
40. Muntz KH, Zhao M, Miller JC. Downregulation of myocardial beta-adrenergic receptors. Receptor subtype selectivity. Circ Res. 1994;74:369–75.
41. Liu J, Nishida M, Inui H, Chang J, Zhu Y, Kanno K, et al. Rivaroxaban suppresses the progression of ischemic cardiomyopathy in a murine model of diet-induced myocardial infarction. J Atheroscler Thromb. 2019;26:915–30.
42. Kondo H, Abe I, Fukui A, Saito S, Miyoshi M, Aoki K, et al. Possible role of rivaroxaban in attenuating pressure-overload-induced atrial fibrosis and fibrillation. J Cardiol. 2018;71:310–9.
43. Ritchie E, Saka M, Mackenzie C, Drummond R, Wheeler-Jones C, Kanke T, et al. Cytokine upregulation of proteinase-activated-receptors 2 and 4 expression mediated by p38 MAP kinase and inhibitory kappa B kinase beta in human endothelial cells. Br J Pharmacol. 2007;150:1044–54.
44. Ramachandran R, Sadofsky LR, Xiao Y, Botham A, Cowen M, Morice AH, et al. Inflammatory mediators modulate thrombin and cathepsin-G signaling in human bronchial fibroblasts by inducing expression of proteinase-activated receptor-4. Am J Physiol Lung Cell Mol Physiol. 2007;292:L788–98.
45. Freund-Michel V, Frossard N. Inflammatory conditions increase expression of protease-activated receptor-2 by human airway smooth muscle cells in culture. Fundam Clin Pharmacol. 2006;20: 351–7.
46. Woodall MC, Woodall BP, Gao E, Yuan A, Koch WJ. Cardiac fibroblast GRK2 deletion enhances contractility and remodeling following ischemia/reperfusion injury. Circ Res. 2016;119:1116–27.
47. Hayashida T, Decaestecker M, Schnaper HW. Cross-talk between ERK MAP kinase and Smad signaling pathways enhances TGF-beta-dependent responses in human mesangial cells. FASEB J. 2003;17:1576–8.
48. Liu X, Hubchak SC, Browne JA, Schnaper HW. Epidermal growth factor inhibits transforming growth factor-beta-induced fibrogenic differentiation marker expression through ERK activation. Cell Signal. 2014;26:2276–83.
49. Kawabata A, Kuroda R, Nakaya Y, Kawai K, Nishikawa H, Kawao N. Factor Xa-evoked relaxation in rat aorta: involvement of PAR-2. Biochem Biophys Res Commun. 2001;282:432–5.
50. Cicala C, Pinto A, Bucci M, Sorrentino R, Walker B, Harriot P, et al. Protease-activated receptor-2 involvement in hypotension in normal and endotoxemic rats in vivo. Circulation. 1999;99:2590–7.
51. Maruyama K, Kagota S, McGuire JJ, Wakuda H, Yoshikawa N, Nakamura K, et al. Enhanced nitric oxide synthase activation via protease-activated receptor 2 is involved in the preserved vasodilation in aortas from metabolic syndrome rats. J Vasc Res. 2015; 52:232–43.
52. Kagota S, Chia E, McGuire JJ. Preserved arterial vasodilatation via endothelial protease-activated receptor-2 in obese type 2 diabetic mice. Br J Pharmacol. 2011;164:358–71.
53. Hara T, Fukuda D, Tanaka K, Higashikuni Y, Hirata Y, Nishimoto S, et al. Rivaroxaban, a novel oral anticoagulant, attenuates atherosclerotic plaque progression and destabilization in ApoE-deficient mice. Atherosclerosis. 2015;242:639–46.
54. Pham PT, Fukuda D, Yagi S, Kusunose K, Yamada H, Soeki T, et al. Rivaroxaban, a specific FXa inhibitor, improved endothelium-dependent relaxation of aortic segments in diabetic mice. Sci Rep. 2019;9:11206.

55. Moran CS, Seto SW, Krishna SM, Sharma S, Jose RJ, Biros E, et al. Parenteral administration of factor Xa/IIa inhibitors limits experimental aortic aneurysm and atherosclerosis. Sci Rep. 2017; 7:43079.
56. Zuo P, Zuo Z, Zheng Y, Wang X, Zhou Q, Chen L, et al. Protease-activated receptor-2 deficiency attenuates atherosclerotic lesion progression and instability in apolipoprotein E-deficient mice. Front Pharmacol. 2017;8:647.
57. Kurdi M, Booz GW. New take on the role of angiotensin II in cardiac hypertrophy and fibrosis. Hypertension. 2011;57: 1034–8.
58. Zhang R, Zhang YY, Huang XR, Wu Y, Chung AC, Wu EX, et al. C-reactive protein promotes cardiac fibrosis and inflammation in angiotensin II-induced hypertensive cardiac disease. Hypertension. 2010;55:953–60.
59. Ardanaz N, Yang XP, Cifuentes ME, Haurani MJ, Jackson KW, Liao TD, et al. Lack of glutathione peroxidase 1 accelerates cardiac-specific hypertrophy and dysfunction in angiotensin II hypertension. Hypertension. 2010;55:116–23.
60. Zile MR, Baicu CF, Gaasch WH. Diastolic heart failure–abnormalities in active relaxation and passive stiffness of the left ventricle. N Engl J Med. 2004;350:1953–9.